

Assessment of Hepatic Portal Perfusion Using T2* Measurements of Gd-DTPA

Hidemasa Uematsu, MD • Hiroki Yamada, MD • Norihiro Sadato, MD • Satoshi Muramoto, MD
Hiroshi Inoue, RT • Koji Hayashi, RT • Yoshiharu Yonekura, MD • Hirohiko Kimura, MD
Hajime Sakuma, MD • Tetsuya Matsuda, MD • Nobushige Hayashi, MD
Kazutaka Yamamoto, MD • Yasushi Ishii, MD

Recently, perfusion imaging has been of increasing interest in MRI. We applied this method for semiquantitative evaluation of hepatic parenchymal portal blood flow in patients with diffuse liver damage. Twenty patients with diffuse hepatic damage were divided according to the Child's Classification and studied. Gadolinium-diethylenetriamine pentaacetic acid (Gd-DTPA) was administered into the superior mesenteric artery (SMA), and a dynamic series of T2*-weighted fast low angle shot (FLASH) images was obtained. We evaluated relative regional portal blood volume (rrPBV), mean transit time (MTT), and relative regional portal blood flow (rrPBF). The relationship between the rrPBV, rrPBF, and plasma indocyanine green retention rate test at 15 minutes (ICGR₁₅) was also evaluated in 12 patients. Both rrPBF and rrPBV are significantly decreased in Child B & C patients compared with Child A patients. On the other hand, the MTT is significantly prolonged in Child B & C patients compared with Child A patients. Significant correlations were also noted between rrPBF and ICGR₁₅ and between rrPBF and MTT. By means of selective catheterization into the SMA, we were able to estimate rrPBV, rrPBF, and MTT. This method may play a clinical role for assessment of regional portal perfusion in various diseases with diffuse liver damage.

Index terms: Portal vein • Perfusion study • Liver cirrhosis • Portal perfusion • MRI

JMRI 1998; 8:650-654

Abbreviations: CTAP = CT imaging during arterial portography, FLASH = fast low angle shot, Gd-DTPA = gadolinium-diethylenetriamine pentaacetic acid, ICGR₁₅ = indocyanine green retention rate test at 15 minutes, MRAP = MRI during arterial portography, MTT = mean transit time, PET = positron emission tomography, SMA = superior mesenteric artery, ROI = region of interest, rrPBF = relative regional portal blood flow, rrPBV = relative regional portal blood volume, TAE = transarterial hepatic embolization.

From the Department of Radiology and Biomedical Imaging Research Center, Fukui Medical School, 23 Shimoaizuki, Matsuoka-cho, Yoshida-gun, Fukui, Japan 910-11 (H.U., H.Y., N.S., Y.Y., H.K., N.H., K.Y., Y.I.); the Department of Radiology, Rakuwakai Otowa Hospital, Kyoto, Japan (S.M., H.I., K.H.); the Department of Radiology, Mie University, School of Medicine, Mie, Japan (H.S.); and the 3rd Division, Internal Medicine, Kyoto University, Kyoto, Japan (T.M.). Received April 29, 1997; revision requested July 1; revision received August 8; accepted August 21. This paper was presented at 4th annual meeting of the International Society for Magnetic Resonance in Medicine, 1996. **Address reprint requests to H.U.**

© ISMRM, 1998

THE HEPATIC BLOOD FLOW is one of the most important factors determining hepatic function (1). In patients with diffuse liver disease such as cirrhosis, hepatic blood flow correlates with the severity of the disease (2). The measurement of regional parenchymal blood flow will be useful to evaluate underlying hepatic dysfunction. In patients with diffuse liver disease such as cirrhosis, the proportion of the hepatic arterial supply increases with decrease in parenchymal portal flow (1,3-5). Transarterial hepatic embolization (TAE) is an important procedure to control hepatocellular carcinoma (6), which is accompanied by cirrhotic changes of varying degrees. Because this procedure inevitably reduces arterial blood supply not only to the hepatocellular carcinoma but also to the liver tissue, monitoring portal hemodynamics before the procedure is important to determine its indication. Recently, perfusion imaging by monitoring the capillary transit of an injected contrast agent has been of increasing interest in MRI (7). Paramagnetic lanthanide chelates generate microscopic heterogeneous magnetic fields arising from their magnetic susceptibility, leading to significant signal reduction in T2- and T2*-weighted images. We applied this method for semiquantitative evaluation of hepatic parenchymal portal blood flow by injecting a bolus of gadolinium-diethylenetriamine pentaacetic acid (Gd-DTPA) into the superior mesenteric artery (SMA) in patients with diffuse liver damage.

• MATERIALS AND METHODS

Subjects

Twenty patients with diffuse hepatic damage who were suspected of having hepatocellular carcinoma (18 men and 2 women, 44-80 years of age) were studied. None of these patients had undergone surgical procedures, such as treatment for hepatocellular carcinoma or extrahepatic shunt, before this investigation. After this investigation, all patients received conventional angiography for transarterial embolization. Written informed consent was obtained from all patients before this study.

These patients were divided into two groups according to the Child's Classification (Child A, 14 cases; Child B & C, six cases), which provides the prognostic guidance for diffuse hepatocellular diseases according to the level of

Table 1
Child's Classification^a

| Group | A Low Risk | B Moderate Risk | C High Risk |
|-------------------------|------------------|-----------------------|----------------------|
| Total bilirubin (mg/dl) | <2.0 | 2.0-3.0 | >3.0 |
| Serum albumin (g/dl) | >3.5 | 3.0-3.5 | <3.0 |
| Ascites | none | easy to control | difficult to control |
| Encephalopathy | none | minimal | advanced coma |
| Nutrition | excellent | good | poor |

^aChild's Classification uses five parameters.

jaundice, ascites, encephalopathy, serum albumin, and nutrition (Table 1).

MRI Techniques

All examinations were performed with a 1.0-T whole body MRI system (Magnetom 42 SP, Siemens-Asahi, Tokyo, Japan) using a body coil. T1-weighted turbo fast low angle shot (FLASH) images in coronal planes (with the following sequence parameters: TR = 6.5 msec, TE = 3 msec, inversion time = 100 msec, flip angle = 10°, matrix size = 128 × 64, 10-mm thickness, 50-cm field of view) were used to determine the axial slice, including the liver hilum, in which a dynamic series of T2*-weighted axial FLASH images (4 seconds × 25 frames) were obtained (TR = 34 msec, TE = 21 msec, flip angle = 10°, matrix size = 128 × 64, 10-mm thickness, 50-cm field of view).

Patients were instructed to hold their breath for 30 seconds and then to breathe as quietly as possible during the examination.

Study Protocol

The patients had fasted for at least 6 hours before the examination. After the tip of a 5-Fr end-hole angiographic catheter with no metal parts (Terumo, Tokyo, Japan) was placed into the SMA, the patient was transferred to the MRI unit. Gd-DTPA (.1 mmol/kg body weight; Magnevist, Nihon Schering, Osaka, Japan) was administered into the SMA as a bolus 12 seconds after the start of image acquisition. The connecting tube was flushed with a 20-ml saline solution. These injections were performed by one investigator (H.U.). Prostaglandin E1 was not used before this study. In this investigation, we applied the methods such as CT imaging during arterial portography (CTAP) (8), or MRI during arterial portography (MRAP) (9-11). After this investigation, conventional angiography and transcatheter arterial embolization (TAE) were performed on all subjects.

Data Analysis

The regions of interest (ROIs) were placed in the main portal vein (portal input function) and hepatic parenchyma (right lobe). To minimize the effects of hepatic parenchymal hemodynamic inhomogeneities, we placed the ROI in the hepatic parenchyma, making it as large as possible. The measured signal intensity was transformed to $\Delta R2^*$ ($T2^*$ rate change = $\Delta(1/T2^*)$) according to the following relationship:

$$\Delta R2^* = -\ln(S/S_0)/TE$$

where S_0 is precontrast baseline signal intensity and S is signal intensity at time t . The area under the time- $\Delta R2^*$ curve is considered to be proportional to the relative local

blood volume (7). Absolute blood volumes were calculated as the area under the time- $\Delta R2^*$ curve in ROIs and normalized to the input function (12). We applied this equation for a semiquantitative measurement of the local hepatic portal perfusion. To determine relative regional blood volume, we numerically integrated the data during the first transit of Gd-DTPA after curve fitting of the measured data with a γ -variate function to avoid the recirculation effect. We defined relative regional portal blood volume (rrPBV) and relative regional portal blood flow (rrPBF) as the following relationship (7):

$$rrPBV = \frac{\int \Delta R2^* (\text{hepatic parenchyma}) dt}{\int \Delta R2^* (\text{portal vein}) dt}$$

$$rrPBF = \frac{rrPBV}{MTT}$$

We defined mean transit time (MTT) as the following relationship:

$$MTT = \frac{\int_0^{\infty} \Delta R2^* (\text{portal vein}) dt - \int_0^{t-\Delta R2^* \text{ max.}} \Delta R2^* (\text{hepatic parenchyma}) dt}{\Delta R2^* \text{ max (hepatic parenchyma)}}$$

where $\Delta R2^*$ max is the maximum height of the time- $\Delta R2^*$ curve (hepatic parenchyma). This relationship is described in detail by Ishii and MacIntyre (13).

Correlation

A plasma indocyanine green retention rate test at 15 min ($ICGR_{15}$) was performed before this investigation in 12 patients. The relationship between the rrPBV, rrPBF, and $ICGR_{15}$ was also evaluated in these 12 patients.

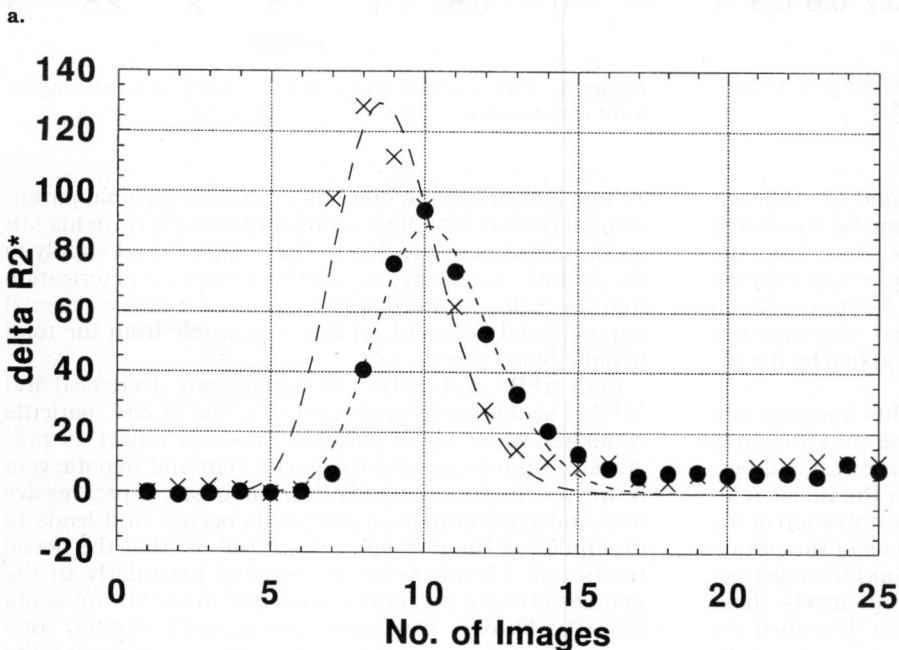
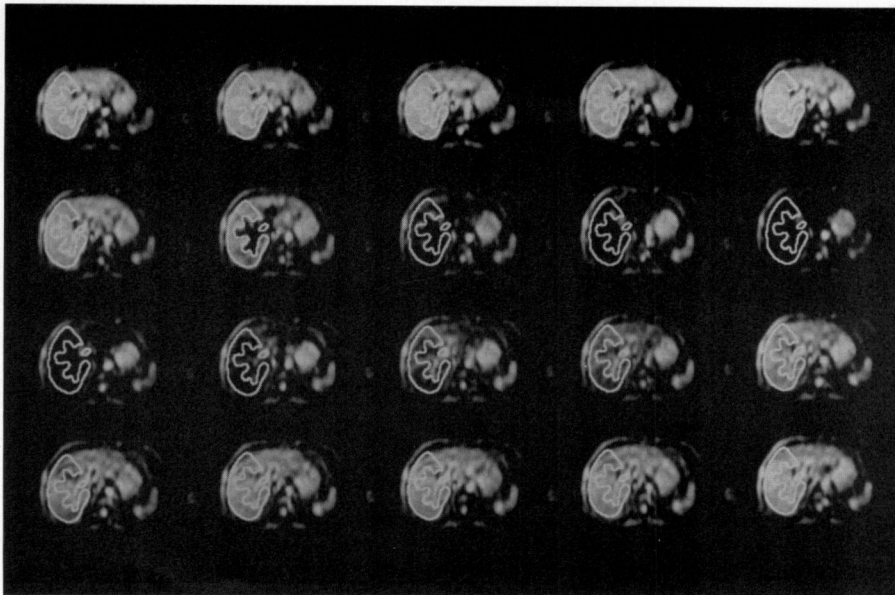
Statistical Analysis

All results are expressed as mean \pm SD. Statistical review of rrPBV, MTT, and rrPBF between Child A and Child B & C was performed with the use of the Mann-Whitney U test. The relationship between rrPBV, rrPBF, and the $ICGR_{15}$ was analyzed by simple regression with Pearson's correlation coefficient. A P value of less than .05 was considered to be statistically significant.

RESULTS

Three patients were not able to suspend respiration sufficiently and were omitted from further analysis. In the studies of the other 17 subjects (Child A, 12 patients; Child B & C, five patients), the ROIs were satisfactorily placed in the main portal vein and hepatic parenchyma. After the bolus administration of Gd-DTPA into the SMA, entry of the contrast agent into the portal vein caused rapid signal attenuation, followed by the signal attenuation in the hepatic parenchyma (Fig. 1a). The maximum signal reduction in the hepatic parenchyma was delayed compared with that of the portal vein. Typical time- $\Delta R2^*$ curves in the portal vein and the hepatic parenchyma are demonstrated in Figure 1b.

Both rrPBF and rrPBV are significantly decreased in Child B & C patients compared with Child A patients (Table 2; $P < .05$, Mann-Whitney U test). The MTT is significantly prolonged in Child B & C patients compared with Child A patients (Table 2; $P < .05$, Mann-Whitney U test). Significant correlation was also noted between rrPBV and $ICGR_{15}$ (Fig. 2; $r = .62$, $P < .05$), and rrPBF and $ICGR_{15}$ (Fig. 3; $r = .67$, $P < .05$).



• **DISCUSSION**

Measurement of portal blood flow is clinically important to evaluate diffuse liver disease. Recently, Doppler ultrasound techniques (14) and phase-contrast cine MR angiography (15) are reported to be useful as noninvasive measurements of the portal blood flow. However, these techniques allow evaluation of portal blood flow only in the main portal vein, not parenchymal perfusion. In some patients, Doppler assessment of the portal venous system is compromised due to intestinal gas, a large amount of fat in the obese patients, and lack of patient cooperation. Moreover, these techniques do not account for an extra hepatic shunt.

Scintigraphy with radioactive colloid (16) and ultrafast CT scan with intravenous injection of the contrast agents (3) can measure hepatic parenchymal arterial and portal blood flow separately and simultaneously. These meth-

Figure 1. (a) Dynamic series of T2*-weighted axial FLASH images of every 4 seconds (TR = 34 msec, TE = 21 msec, flip angle = 10°, matrix size = 128 × 64, 10-mm thickness, 50-cm field of view, 4 second × 25 frames) obtained during first transit of the Gd-DTPA (.1 mmol/kg body weight) in a Child A patient. Twenty of 25 images are shown. After the bolus administration of Gd-DTPA into the SMA, the signal reduction in the hepatic parenchyma was delayed compared with that of the portal vein. The overlaid ROIs are used to calculate the portal input function and hepatic parenchymal perfusion, respectively. (b) Typical time- $\Delta R2^*$ curves of the contrast agent in the same patient. The portal vein is represented by (x) and the hepatic parenchyma is represented by (•). rrPBV = .73, MTT = .27 minute, rrPBF = 2.71.

Table 2
Values of rrPBV, MTT and rrPBF^a

| | Child's A | Child's B & C | |
|-----------|-------------|---------------|----------------|
| rrPBV | .69 ± .21 | .47 ± .13 | <i>P</i> < .05 |
| MTT (min) | .46 ± .24 | .93 ± .21 | <i>P</i> < .05 |
| rrPBF | 1.97 ± 1.21 | .55 ± .31 | <i>P</i> < .05 |

^aMean ± SD.

ods require the complicated curve analysis of the radioactivity or density to dissect the arterial and portal phase. Positron emission tomography (PET) with ¹⁵O-water can also measure the hepatic arterial and portal blood flow separately and simultaneously (4). However, it requires a cyclotron for the production of an extremely short half-life (2 minutes) tracer.

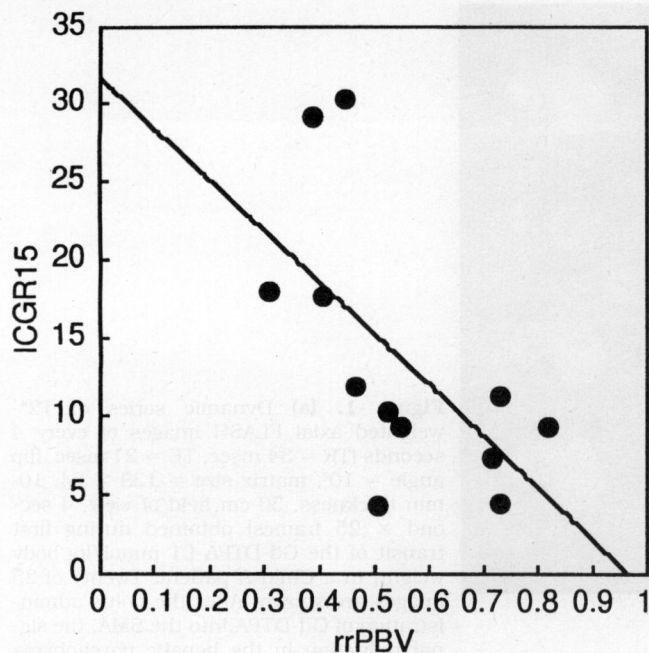


Figure 2. Plot of rrPBV versus ICGR₁₅. rrPBV showed a significant correlation ($r = .62$, $P < .05$) with ICGR₁₅.

With the arterial catheter technique and Xe-133, parenchymal hepatic portal blood flow can be measured separately (5). To measure portal blood flow from the washout curves of Xe-133, the radiotracer was injected into the proper hepatic artery followed by its occlusion with an inflated balloon (5). This method may measure nonphysiologic portal hemodynamics modified by the occlusion of the hepatic artery.

Dynamic T2*-weighted MRI with a bolus injection of a susceptibility contrast agent used in the present study has first applied in the brain to quantitate regional perfusion (17,18). This method is based on the linear relationship between $\Delta R2^*$ and the local concentration of the paramagnetic contrast agents on the basis of the principles of the indicator dilution theory for nondiffusible tracers. It was shown that the normal brain meets these conditions (19). Recent reports have also described the effectiveness of magnetic susceptibility contrast media for quantitation of myocardial perfusion (20–22).

The organization of the vasculature bed in the liver is quite different from that of the normal brain. No tight junction exists between endothelial cells. Holes are frequent in endothelial cells, and there is no anatomically identifiable basement membrane under the sinusoidal lining cells. These three structural attributes allow direct access of plasma from the sinusoidal lumen to the surface of hepatocytes (23). Some proportion of Gd-DTPA is likely to move into the extravascular space (space of Disse) during the first transit. In this study, we defined effective portal capillary blood space as including both intravascular space and the space of Disse.

A previous animal study showed that the signal intensity of the myocardium was reduced by the contrast agent in a dose-dependent manner in both normal and ischemic rats. The plot of the changes in $\Delta R2^*$ versus the injected dose of contrast agent can be plotted well in a straight line (20). These results verify that semiquantitative measurement of local portal perfusion is feasible with dynamic susceptibility contrast-enhancing imaging.

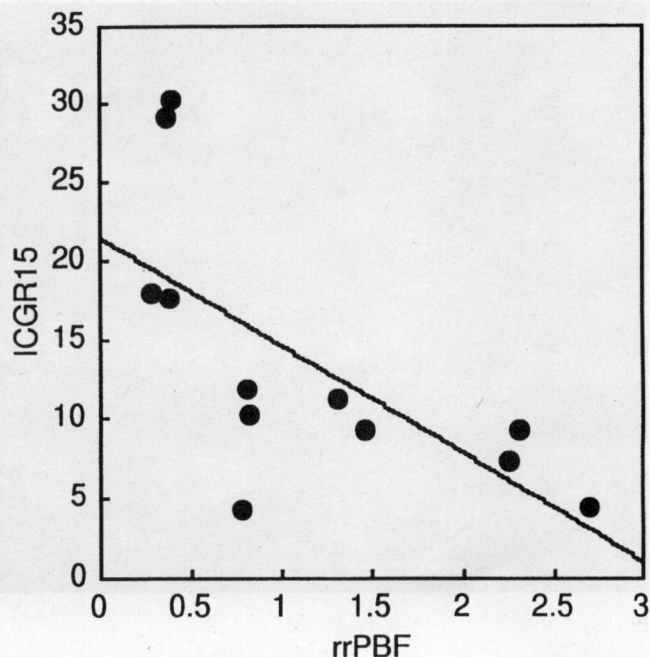


Figure 3. Plot of rrPBF versus ICGR₁₅. rrPBF showed a significant correlation ($r = 0.67$, $P < .05$) with ICGR₁₅.

To our knowledge, no one has evaluated regional parenchymal portal blood flow semiquantitatively by using MR studies. This is partly due to the complex dual supply to the hepatic parenchyma. With selective catheterization into the SMA, we were able to estimate relative regional parenchymal portal blood flow separately from the total hepatic blood flow.

Both rrPBF and rrPBV are significantly decreased and MTT is significantly prolonged in Child B & C patients compared with Child A patients. This may reflect the progressive fibrosis around the portal vein and hepatic vein branches. In patients with liver cirrhosis, a progressive loss and regeneration of liver cells occurs and leads to disruption of the normal architecture, so that the portal tracts and hepatic veins are spaced irregularly in the nodules of surviving parenchyma and in the fibrous septa (23). The fibrosis also causes intrahepatic shunts, such as portocaval and arterioportal shunts, reducing the parenchymal portal flow.

Other than these pathologic changes intrinsic to the cirrhosis, portal hemodynamic alterations are caused by surgical interventions such as transcatheter arterial embolization, hepatic surgical resection, and shunt placement (24). None of these patients had undergone any surgical procedure before the MRI. Therefore, fibrosis mainly affects the portal hemodynamic alterations in this present study.

In this present study, the relationship between the rrPBV, rrPBF, and ICGR₁₅ showed significant correlation. Because ICGR₁₅ is a measure of total hepatic blood flow (25–27) and that portal blood flow is the main determinant of the total hepatic blood flow, this result underscores the feasibility of our method. On the other hand, ICGR₁₅ cannot separately evaluate the portal and arterial blood flow; hence, it is insufficient to determine indications of a transcatheter arterial embolization of the liver.

Several limitations in our method exist. The placement of a catheter in the SMA is invasive. The use of this method must be limited to just before the embolization

procedure. Breath-holding is required to obtain a clear MR image and may affect the portal blood flow by the increased abdominal pressure. This point requires further investigation.

In conclusion, T2*-weighted FLASH imaging with a magnetic susceptibility contrast agent displays the first passage of the contrast material through the hepatic parenchyma. The method potentially provides information about local parenchymal portal perfusion in diffuse liver disease.

Acknowledgments: The authors thank Akane Kitagawa, MD, Sanae Yamamori, MD, Tetsutaro Sakaguchi, MD, Masaki Kobayashi, MD, Takahiko Kosuga, MD, and Kiichiro Watanabe, MD, of Rakuwakai Otowa Hospital, for their many helpful discussions.

References

1. Schenk WG, McDonald JC, McDonald K, Drapanas T. Direct measurement of hepatic blood flow in surgical patients with related observations on hepatic flow dynamics in experimental animals. *Ann Surg* 1962; 156:463-471.
2. Carter JH, Welch CS, Barron RE. Changes in the hepatic blood vessels in cirrhosis of the liver. *Surg Gynecol Obstet* 1961; 113:133-137.
3. Blomley MJK, Coulden R, Dawson P, et al. Liver perfusion studied with ultrafast CT. *J Comput Assist Tomogr* 1995; 19:424-433.
4. Taniguchi H, Oguro A, Takeuchi K, et al. Difference in regional hepatic blood flow in liver segments — non-invasive measurement of regional hepatic arterial and portal blood flow in human by positron emission tomography with H₂¹⁵O-. *Ann Nucl Med* 1993; 7:141-145.
5. Yasuhara Y, Miyauchi S, Hamamoto K. A measurement of regional portal blood flow with Xe-133 and balloon catheter in man. *Eur J Nucl Med* 1989; 15:346-350.
6. Yamada R, Sato M, Kawabata M, et al. Hepatic artery embolization in 120 patients with unresectable hepatoma. *Radiology* 1983; 148:397-401.
7. Rosen BR, Belliveau JW, Chien D. Perfusion imaging by nuclear magnetic resonance. *Magn Reson Q* 1989; 5:263-281.
8. Matsui O, Kadoya M, Suzuki M, et al. Work in progress: dynamic sequential computed tomography during arterial portography in the detection of hepatic neoplasms. *Radiology* 1983; 146:721-727.
9. Pavone P, Giuliani S, Cardone G, et al. Intraarterial portography with gadopentetate dimeglumine: improved liver-to-lesion contrast in MR imaging. *Radiology* 1991; 179:693-697.
10. Soyer P, Laissy JP, Sibert A, et al. Hepatic metastases: detection with multisection FLASH MR imaging during gadolinium chelate-enhanced arterial portography. *Radiology* 1993; 189:401-405.
11. Uematsu H, Yamada H, Sadato N, et al. Multiple single sections turbo FLASH MR arterial portography in the detection of hepatic neoplasms. *Eur J Radiol* 1998 (in press).
12. Rempp KA, Brix G, Wenz F, Becker CR, Gückel F, Lorenz WJ. Quantification of regional cerebral blood flow and volume with dynamic susceptibility contrast-enhanced MR imaging. *Radiology* 1994; 193:637-641.
13. Ishii Y, MacIntyre WJ. Analytical approach to dynamic radioisotope recording. *J Nucl Med* 1971; 12:792-799.
14. Kawasaki T, Moriyasu F, Kimura T, Someda H, Fukuda Y, Ozawa K. Changes in portal blood flow consequent to partial hepatectomy: doppler estimation. *Radiology* 1991; 180:373-377.
15. Burkart DJ, Johnson CD, Morton MJ, Ehman RL. Phase-contrast cine MR angiography in chronic liver disease. *Radiology* 1993; 187:407-412.
16. Sarper R, Fajman WA, Rypins EB, et al. A noninvasive method for measuring portal/ total hepatic blood flow by hepatosplenic radionuclide angiography. *Radiology* 1981; 141:179-184.
17. Rosen BR, Belliveau JW, Vevea JM, Brady TJ. Perfusion imaging with NMR contrast agents. *Magn Reson Med* 1990; 14:249-265.
18. Edelman RR, Mattle HP, Atkinson DJ, et al. Cerebral blood flow: assessment with dynamic contrast-enhanced T2*-weighted MR imaging at 1.5T. *Radiology* 1990; 176:211-220.
19. Belliveau JW, Rosen BR, Kantor HL, et al. Functional cerebral imaging by susceptibility-contrast NMR. *Magn Reson Med* 1990; 14:538-546.
20. Wendland MF, Saeed M, Masui T, Derugin N, Higgins CB. First pass of an MR susceptibility contrast agent through normal and ischemic heart: gradient-recalled echo planar imaging. *JMRI* 1993; 3:755-760.
21. Sakuma H, O'Sullivan M, Lucas J, et al. Effect of magnetic susceptibility contrast medium on myocardial signal intensity with fast gradient-recalled echo and spin-echo MR imaging: initial experience in humans. *Radiology* 1994; 190:161-166.
22. Saeed M, Wendland MF, Lauerma K, et al. First-pass contrast-enhanced inversion recovery and driven equilibrium fast GRE imaging studies: detection of acute myocardial ischemia. *JMRI* 1995; 5:515-523.
23. McGee J. The liver and biliary system. In: McGee J, Isaacson PG, Wright NA, eds. *Oxford textbook of pathology*, vol. 2a. Oxford: Oxford University Press, 1992; 1287-1291.
24. Chin N, Ohnishi K, Iida S, Nomura F. Role of intrahepatic portal-systemic shunts in the reduction of portal blood supply to liver cell in cirrhosis. *Am J Gastroenterol* 1988; 83:718-722.
25. Caesar JS, Shaldon L, Chiandussi L. Use of indocyanine green in measurement of hepatic blood flow and as a test of hepatic function. *Clin Sci* 1961; 21:43-57.
26. Wiegand BD, Ketterer SG, Rappaport E. The use of indocyanine green for the evaluation of hepatic function and blood flow in man. *Am J Dig Dis* 1960; 5:427-436.
27. Wynne HA, Goudevenos J, Rawlins MD. Hepatic drug clearance: the effect of age using indocyanine green as a model compound. *Br J Clin Pharmacol* 1960; 30:634-637.